

# Local Padding in Patch-Based GANs for Seamless Infinite-Sized Texture Synthesis

Alhasan Abdellatif<sup>\*1</sup>, Ahmed H. Elsheikh<sup>†1</sup>, and Hannah Menke<sup>‡1</sup>

<sup>1</sup>Heriot-Watt University

May 15, 2024

## Abstract

Texture models based on Generative Adversarial Networks (GANs) use zero-padding to implicitly encode positional information of the image features. However, when extending the spatial input to generate images at large sizes, zero-padding can often lead to degradation of quality due to the incorrect positional information at the center of the image and limit the diversity within the generated images. In this paper, we propose a novel approach for generating stochastic texture images at large arbitrary sizes using GANs model that is based on patch-by-patch generation. Instead of zero-padding, the model uses *local padding* in the generator that shares border features between the generated patches; providing positional context and ensuring consistency at the boundaries. The proposed models are trainable on a single texture image and have a constant GPU scalability with respect to the output image size, and hence can generate images of infinite sizes. We show in the experiments that our method has a significant advancement beyond existing texture models in terms of the quality and diversity of the generated textures. Furthermore, the implementation of local padding in the state-of-the-art super-resolution models effectively eliminates tiling artifacts enabling large-scale super-resolution. Our code is available at [https://github.com/ai4netzero/Infinite\\_Texture\\_GANs](https://github.com/ai4netzero/Infinite_Texture_GANs).

**Keywords:** Generative Adversarial Networks (GANs), Texture Synthesis, Large-scale generation.

---

<sup>\*</sup>a.abdellatif@hw.ac.uk

<sup>†</sup>a.elsheikh@hw.ac.uk

<sup>‡</sup>h.menke@hw.ac.uk

# 1 Introduction

Texture synthesis refers to the process of generating arbitrary-size textures that are visually similar to a given input example, while also being diverse and not a simple duplication of the input. This problem has numerous applications in fields such as gaming, virtual reality and graphic design, where high-quality textures are critical for creating realistic and visually appealing environments. The use of Generative Adversarial Networks (GANs) [1] in generating realistic textures has been widely explored. Several methods have been proposed for this task, including Spatial GAN [2], PSGAN [3], adversarial expansion [4] and SinGAN [5]. However, using these models to generate arbitrary large-scale textures while maintaining their quality and diversity is not trivial.

Expanding the size of the input latent space of these models is always limited by the GPU memory that restricts the output image size. In addition, when using zero-padding, extending the input dimensions results in degraded quality due to the propagation of incorrect positional information. Furthermore, zero-padding can cause limited variability at the corners of the generated images and can often result in tiling or seaming artifacts between the generated patches in incremental generation, i.e., patch-by-patch generation. This problem is more pronounced in image translational tasks, where several work tried to alleviate the discontinuities at the patch borders either by post-training tiling [6] or integrating the tiles into training [7].

To address these challenges, we propose a patch-based GAN model with a novel padding method that is capable of synthesizing stochastic textures of infinite size and that is trainable on a single texture image. Because of the self-similarity and homogeneity within texture images, it is sufficient to maintain its structure by sharing local information only. Relying on this concept, our model uses *local padding*, instead of zero-padding, where the inputs to the generator’s convolutional layers are padded with content from neighbouring patches to ensure seamless concatenation. During training, the model generates locally-correlated small-size patches and learns to stitch them together based on the padded information provided. Using incremental generation, in the inference time, we can extend the generation to arbitrary large sizes while maintaining the texture structure and diversity.

The main contribution of the papers:

- We propose *local padding* as a new way of padding the inputs before convolutional operations that allows seamless patch-by-patch texture synthesis.
- We demonstrate that our trained models are capable of generating higher-quality texture images than existing models while maintaining the fine details and variability exhibited by the original examples and that they are scalable to any resolution by incremental generation.
- We also show that local padding can be used in the state-of-the-art super-resolution models, such as Real-ESRGAN [8], to avoid tiling artifacts when super-resolving large inputs.

The rest of the paper is organized as follows: in the next section we review related work. In section 3, we discuss the new developed patch-by-patch generation with local padding. In section 4, we show and discuss the results. Finally, a conclusion is given in section 5.

## 2 Related Work

**GANs for texture synthesis.** Generative Adversarial Networks (GANs) [1] have gained significant attention in recent years due to their ability to generate realistic images. They have found numerous applications in computer vision, ranging from image-to-image translational tasks [9–11], super-resolution [8, 12, 13], and image in-painting [14, 15]. They have also shown great potential for generating realistic textures, where the challenge is to generate samples of arbitrary large sizes while preserving the coherence and consistency of the given example. Spatial GAN [2] builds upon the DCGANs architecture [16] by transforming the generator and discriminator into fully convolutional networks, where the output texture image can be expanded in size by expanding the spatial input. Periodic Spatial GAN (PSGAN) [3] proposes to generate textures with periodic patterns by incorporating a periodic input into the generator network. Adversarial expansion [4] trains a GAN model to double the size of the input texture image. However, expanding the input size of the latent space leads to incorrect positional encoding in the generated images and hence degrades the quality. Moreover, adversarial expansion model did not parametrize the stochasticity of the texture, and instead performed diversification by shuffling and cropping.

SinGAN [5] trains multi-scale generators to generate realistic images, including textures, from a single input image. TileGAN [17] designed a tiling framework to synthesize large-scale texture images based on neighbourhood similarity search. While these models successfully generated high-resolution images of textures, the zero-padding used led to limited spatial variability around the boundaries of the generated images in case of SinGAN and visible artifacts between the tiles with TileGAN. In addition, the TileGAN method required storing latents representation of large number of generated examples to be searched for similarity matching which is time-consuming. Compared to previous texture work, our method refrains from using zero-padding and introduces *local padding* in the generator, which enables seamless generation of texture images via patch-by-patch generation and maintains the stochastic nature of the texture.

**Large-Scale Generation.** In [18–21], CNN-based GANs were trained to generate images of high-resolution. HiTGAN [22] used self-attention to capture the local and global dependencies in a transformer-based GAN to generate high-resolution images. However, generating images of large arbitrary sizes using these models is not directly possible, as they are trained on images of finite resolutions, and training on extremely large sizes is constrained by limited resources. The most related work to the proposed local padding is StreamingCNN [23], where the convolutional operations are performed on small tiles

of the input image for image recognition tasks. But our work is different in that global operations such as batch normalization are still computed within each patch which is a limitation in StreamingCNN.

**Incremental Generation.** In patch-by-patch generation, the model synthesizes one small patch at a time, then correlated patches are assembled to form a larger image. This allows the model to generate images with an infinite size and avoid the problem of limited resources and the training instabilities associated with generating a large image in a single forward pass [18]. COCOGAN [24] trains a GAN model that conditions image patches on coordinates and then assembles patches that share a global latent vector. This allowed for limited extrapolation of the images by extending the coordinates. InfinityGAN [25] then extended the method to natural images by employing a padding-free generator. Similar to our work, they removed zero-padding in their generator and instead padded the inputs with neighbouring content, which allowed for seamless concatenation. To model the position of the patches, (e.g., sky, land), they employed an implicit neural function with CoordConv [26], where the hidden representations are concatenated with positional embeddings.

LocoGAN [27] trains fully convolutional GANs on sub-images instead of the full image and uses coordinates to inform the model which part of the image is being generated. ALIS [28] used a spatially-equivariant generator where they modified the AdaIN algorithm [29] such that the modulating parameters are spatially-interpolated. This approach enabled the generation and assembly of vertical patches of natural scenes. However, the model suffers from content repetition when the global anchors do not change fast enough to allow for variations. In addition, the padding used in the generation led to blocky artifacts and discontinuity between the generated patches. Unlike natural images that require global coordination between the different patches, texture images exhibit a high degree of locality and self-similarity. With local padding applied to all levels in the generator, our model can capture the local structure of the texture without the need for explicit global coordination between the patches.

### 3 Methodology

The proposed method relies on homogeneity and self-similarity within texture images. This property allows us to synthesize texture patches using only information from the neighbouring patches. An overview of the method is presented in Figure 1. Following [2], both the generator and discriminator are fully convolutional neural networks. Multiple patches are randomly cropped from the single texture image and are passed to the discriminator. However, instead of expanding the spatial input noise to generate larger images, we limit the generator network to generate, in parallel,  $N \times N$  small-size patches, each patch is of size  $h \times w$ . The model learns to seamlessly assemble these patches together based on shared information between the patches. Since most texture images are stationary and homogenous, it is sufficient to capture the local spatial structure by passing border features of the patches. For this reason, we pad the input

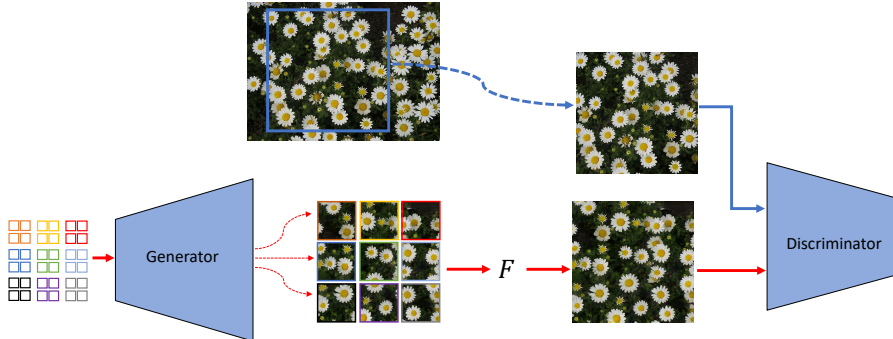


Figure 1: Overview of the training process for the proposed method. An image patch is cropped randomly from the single texture image and is passed to the discriminator. The generator takes a spatial input  $z_i$  to generate, in parallel,  $3 \times 3$  small-size patches  $x_i = G(z_i) \forall i \in 1 \dots 9$  that are passed to an assembling function  $F$  to form a larger image  $X = F(x_1, \dots, x_9)$ . The assembled image is then passed to the discriminator for evaluation. The blue arrows indicate the real patches path while the red arrows indicate the generated patches path. The spatial size of each  $z_i$  is  $4 \times 4$ , although it is shown as  $2 \times 2$  in the figure for simplicity.

to the convolutional layers in the generator with content from the neighbouring patches, through *local padding*, instead of the conventional zero-padding. The assembling is done by indexing each patch  $x_i$  and concatenating these patches into one image where  $X = F(x_1, \dots, x_{N^2})$ . Here  $F$  is a simple concatenation function, which is then passed to the discriminator.

**Local Padding.** We introduce *local padding* as a type of padding used in patch-based generation, where the inputs to the convolutional operations at all levels in the generator are padded by the boundary content of neighbouring patches. Typically, padding involves adding extra rows and columns of zeros around the input image or feature map to ensure that the convolutional filters can be applied to the edges. However, using zero-padding in a patch-by-patch generator results in visible seams between the concatenated patches. This mismatch occurs because the pixels at the boundaries may not align perfectly with those in the neighbouring patches.

Local padding tries to address this issue by using the values from the input or the feature maps of the adjacent patches to fill in the padded pixels, as depicted in Figure 2. Global operations such as batch-normalization and nearest neighbour up-sampling are still performed on each patch independently. This ensures that the convolutional filters can be applied to the edges of the feature maps without losing border information. In addition, sharing the padding between the patches and assemble them together during training allows the model to learn to seamlessly stitch the patches based on the shared padding. Padding

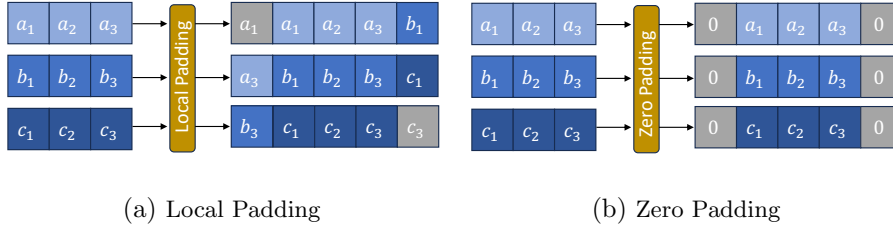


Figure 2: Comparison between local padding and zero-padding applied to a batch of 3 inputs, each of size  $1 \times 3$ . a) In local padding, the features of neighbouring patches are used to pad each input before passing to a convolutional layer. Replicate padding is used for the border pixels in the outer patches as there is no neighbouring content. b) Zero-padding simply pads each input with zero values, leading to border inconsistency when assembling the patches together.

from neighbouring patches is similar to [25], however we perform the padding at all layers in the generator not just at the input layer. This provides the neighbouring patches context for all levels when generating the local patch and passes the positional information without the need for explicit coordination.

The amount of padding applied depends on the size and the number of the convolutional filters used. For example, a  $4 \times 4$  input is padded with 1 value at both dimensions to be of size  $6 \times 6$  before passing it to a  $3 \times 3$  convolution. For the outer patches, we use replicate padding to extend the input along the edges, as we do not have neighbouring patches to provide padding values. This approach lends itself to an easy extension to infinite image generation as we will detail next.

**Scaling to Infinite Sizes.** We explain the scaling process for 1-dimensional patches in the horizontal direction in Figure 3. First, using patch generation with local padding, we can generate an image  $X_1$  which is a concatenation of the patches  $x_1, x_2$  and  $x_3$ . The same process is repeated to generate a new image  $X_2$ . However, the rightmost patch in  $X_1$  (i.e.,  $x_3$ ), which was generated using replicate padding, will be regenerated in  $X_2$  using local padding, i.e., by padding from features in  $x_2$  and  $x_4$ , so that the regenerated patch  $x_3^*$  is consistent with both images.  $x_3$  is then dropped and the remaining patches are concatenated with the patches in  $X_1$  to form a larger image  $X_3 = F(x_1, x_2, x_3^*, x_4, x_5)$ . In the last two rows of the figure, we show examples in which the leftmost patch in  $X_2$  is similar to the rightmost patch in  $X_1$ , except that the right side has been modified with local padding to match the interior patches in  $X_2$ . This incremental process can be repeated in the two dimensions to generate images of infinite sizes while maintaining constant GPU memory and avoiding visible seams or artifacts between the patches.

Although, this autoaggressive approach requires caching some values of the feature maps to be used for local padding in the next steps, only a small frac-

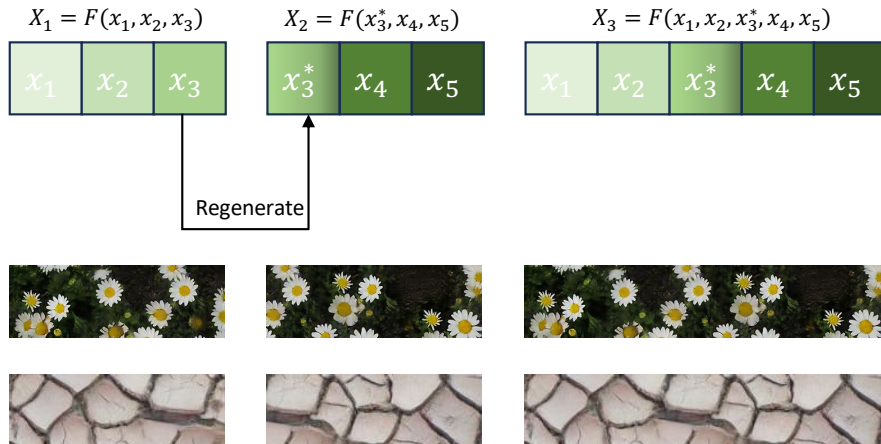


Figure 3: Scaling in the horizontal direction: (Top) Two images  $X_1$  and  $X_2$ , each composed of  $1 \times 3$  generated patches, where the rightmost patch in  $X_1$  is regenerated to match the interior patches of  $X_2$  (i.e.,  $x_3$  is regenerated to be consistent with  $x_4$ ).  $X_3$  is then formed by concatenating  $X_2$  with  $X_1$  patches after dropping  $x_3$ . (Bottom) Two examples of generated texture demonstrate the horizontal scaling process, where the rightmost part of the first column has been regenerated with local padding to match the parts with the images in the second column.

tion is required to be stored since we need border values for padding. This is in contrast to other methods that scale with GPU memory, which can quickly become memory-intensive and limit the size of the textures that can be generated as shown in Figure 4. While the proposed method maintains a constant GPU memory requirement regardless of the generated image size, other methods, PSGAN [3], Adversarial Expansion [4], and SinGAN [5], exhibit a direct and proportional growth in GPU memory consumption relative to the image size. Table 1 presents a comparison between the developed method and other related GANs work based on GPU scalability, the use of coordinates, the use of zero-padding, and whether they are trainable on single images.

## 4 Experiments

### 4.1 Experiment Setup

The training examples used in the experiments were obtained from the supplementary materials in [4]<sup>1</sup>. We selected the images such that they are homoge-

<sup>1</sup>The examples can be found at: [https://github.com/jessemelpolio/non-stationary-texture\\_syn](https://github.com/jessemelpolio/non-stationary-texture_syn)

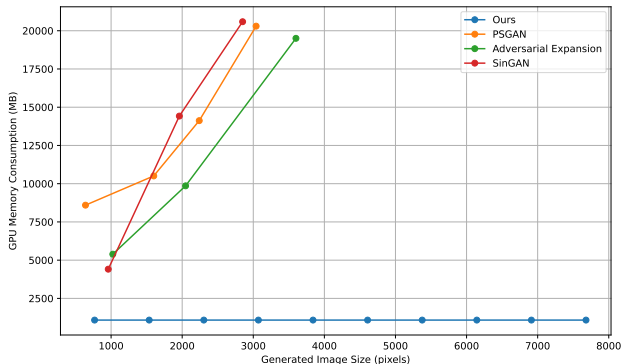


Figure 4: Comparison between the proposed method, PSGAN [3], adversarial expansion [4], and SinGAN [5] based on the GPU memory required to generate images with different sizes. The evaluation was conducted on a single GPU with 24GB of RAM. Notably, the proposed patch-by-patch method maintains a constant GPU memory requirement across all sizes, in contrast to the other methods, where the required GPU memory increases with the size of the generated image.

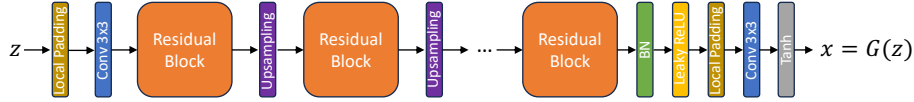
GANs Method	Constant GPU Scalability	Coordinate-free	Avoids zero-padding	Single-image
PSGAN [3]	✗	✓	✗	✓
SinGANs [5]	✗	✓	✗	✓
Adversarial Expansions [4]	✗	✓	✗	✓
LocoGAN [27]	✗	✗	✗	✓
ALIS [28]	✓	✗	✗	✗
InfinityGAN [25]	✓	✗	✓	✗
Ours	✓	✓	✓	✓

Table 1: Comparison of various GANs methods focusing on GPU scalability, coordinate-free implementation, padding-free processing, and suitability for generating single images.

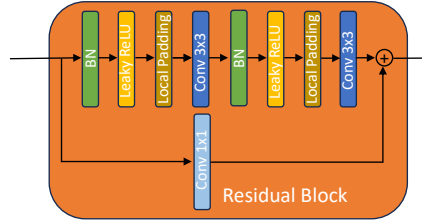
neous and stationary in nature. This is because the developed patch-by-patch approach cannot handle non-stationary patterns.

The generator network is built using ResNets blocks [30] with batch-normalization and nearest neighbour upsampling operations. In addition, we modified the generator to be a fully convolutional network similar to [2, 3], removed all zero-padding following [25], and used local padding before every convolutional layer instead. The architecture of the generator is shown in Figure 5, where the spatial input  $z$  is passed through successive residual blocks interleaved by upsampling layers. We used a PatchGAN discriminator [31, 32], which is designed to provide a more fine-grained evaluation of the generated images by focusing on the local features of the image rather than the global features. Similar to [3], we removed the normalization layers in the discriminator and found this to be more stable and boosted performance when training on a single image. The GANs model is trained with the non-saturating logistic loss with





(a) Generator Architecture.



(b) Residual Block

Figure 5: The architecture of the generator network. The generator takes a spatial noise input  $z$  and successively upsamples it to generate an image patch  $x = G(z)$ . Each  $3 \times 3$  convolutional layer is preceded by local padding where the features are padded with content from neighbouring patches. Batch normalization and upsampling operations are performed on each patch independently.

Image Name (size)	Random Crop	Number of layers in G	Number of layers in D
241 (440 × 614)	192	6	4
34 (450 × 600)	128	5	4
12 (450 × 600)	128	5	3
73 (400 × 600)	128	5	3
417 (192 × 192)	48	4	3

Table 2: Hyper-parameters selected for Experiments: Each row represents a distinct image experiment with the corresponding chosen parameters.

spectral normalization [33] applied to the discriminator weights. The learning rate of both the generator and discriminator is set to 0.0002 and Adam [34] is used for optimization with  $\beta_1 = 0$  and  $\beta_2 = 0.999$ .

During training, we set  $N = 3$ . While other combinations are possible,  $3 \times 3$  is the simplest combination in which the generator can learn the local information between patches (i.e., 1 central and 8 neighbouring patches). During inference, one can set  $N$  to be larger to maximize GPU utilization. The choice of the cropping size depends on the size of the training image, with larger cropping size leading to less diversity, since we are training on a single image. Moreover, the receptive field (RF) of the PatchGAN discriminator is selected to be larger than the size of the texture objects presented in the image so that the model can evaluate them. We present in Table 2, the hyper-parameters used in some of the experiments, where the first column refers to the training image name in the supplementary materials of [4].

Image	PSGAN	SinGAN	Ours
12	0.22	0.27	<b>0.04</b>
34	<b>0.08</b>	0.76	0.09
241	0.12	0.69	<b>0.09</b>
221	0.64	0.43	<b>0.30</b>

Table 3: Comparison of SIFID Values for Different methods (lower is better).

## 4.2 Results

First, we present the visual quality of some generated textures by the proposed method in Figure 6. As observed, the method generates textures with fine details, preserving the overall structure and diversity of the original examples. In Figure 7, we compare between the proposed approach, Adversarial Expansion [4], PSGAN [3], and SinGAN [5] in terms of the quality of the generated texture. As shown, both adversarial expansion and PSGAN generate texture of lower quality since expanding the spatial input of the model changes the positional encoding.

While SinGAN generates reasonable results, it tends to produce smooth images due to the multi-scale training scheme. As a result, some of the high-frequency details in the original example are lost, as shown in the last row. Moreover, because of the zero-padding used in SinGAN, the generated examples exhibit limited variability around the boundaries as shown in Figure 8, where we plot the standard deviation of 50 generated samples computed per pixel.

To generate regular texture, we incorporated periodic inputs proposed in PSGAN in the latent space of our models. In Figure 9, we compare between our method with periodic input, Adversarial Expansion and PSGAN based on generated regular textures. As shown adversarial expansion tries to duplicate the structure presented in the original examples with minimal stochastic variations across the spatial domain. In addition, the zero-padding creates boundary artifacts in the generated textures. PSGAN tends to generate repetitive patterns, diminishing its capacity to produce diverse outputs. On the other hand, the proposed method was able to maintain the regularity of the texture as well as generate diverse and stochastic outputs.

Table 3 presents a quantitative comparison based on SIFID (Single Image FID) [5], a metric used to assess the quality and the diversity of the generated images by calculating the FID distance between feature statistics in the real image and in the generated samples. Average SIFID values are calculated over 50 images for PSGAN [3], SinGAN [5], and our method. As reported, the quality of generated texture images by our method is comparable or better than those generated by PSGAN and SinGAN in most cases. SinGAN tends to have large SIFID values as they have limited variability around the corners of the generated images.

**Local Padding in Super-Resolution models.** Super-resolution based

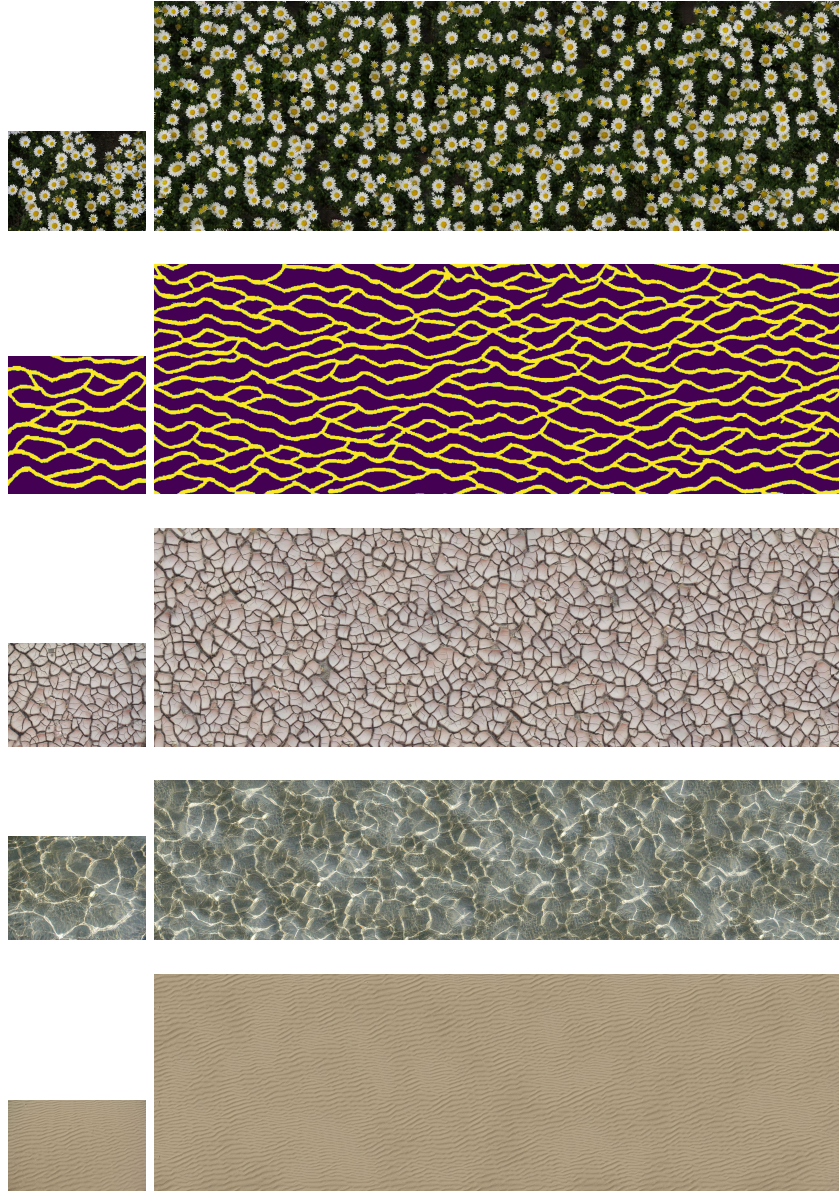


Figure 6: Examples of texture images generated by the proposed method (right column) given the source texture (left column).

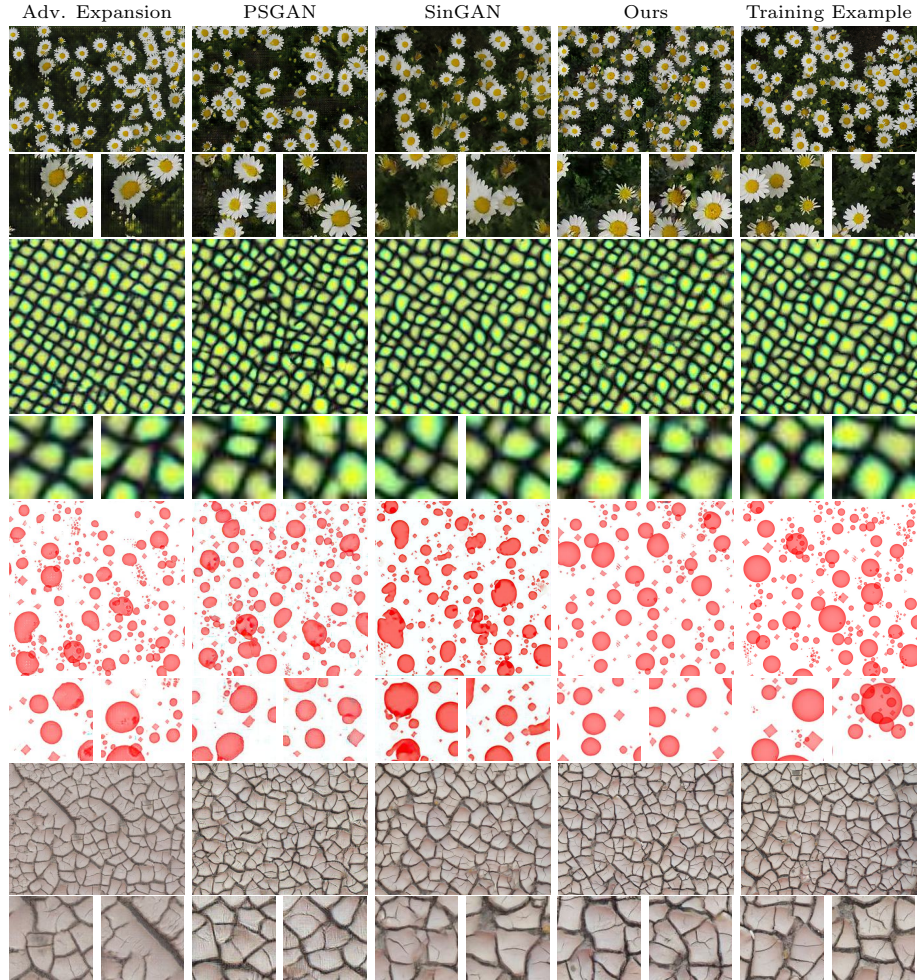


Figure 7: Qualitative comparison between texture generation models based on GANs. For each training example, we show the generated images followed by the corresponding patches for closer examination.

on deep learning models has been an active area of research in the last few years, where the models learn to reproduce the high-frequency details lost in compressed, noisy or blurry images. However, super-resolving large images is limited by the GPU memory, and hence tiling is often used where the large input image is broken down into smaller overlapping tiles or patches. Each tile is processed independently, and the outputs are stitched back together to form the final large image. However, seaming artifacts can appear when assembling

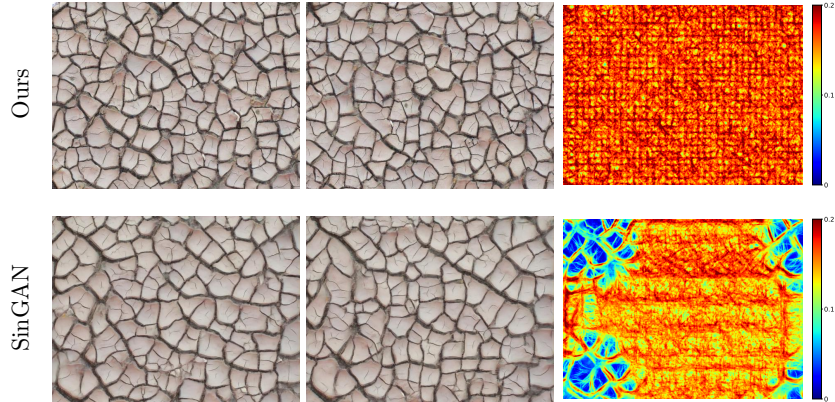


Figure 8: Diversity comparison between our model and SinGAN. The first two columns show two examples generated by our trained model and SinGAN, the last column shows the per-pixel standard deviation computed over 50 samples.

the patches together due to mismatches around the boundaries. To address this problem, we apply local padding in the state-of-the-art Real-ESRGAN [8] model.

Since no global operations is used in the Real-ESRGAN generator (e.g., no batch normalization), we can apply the method directly to the pre-trained model by dropping all the zero paddings and instead use local padding. In Figure 10, we used Real-ESRGAN to super-resolve images using both tiling with different overlapping sizes and local padding. Although increasing the overlapping size between the patches smooths down the discontinuities, the cutting lines are inevitable. On the other hand, local padding resulted in no discontinuity between the patches and produced details similar to the single forward pass to the model.

**Ablation study.** To evaluate the effectiveness of the method, we conducted an ablation study where we ablated the local padding and replaced it with the conventional zero-padding. Figure 11 shows examples of images generated using zero-padding where noticeable seams and discontinuities become apparent between patches, disrupting the visual coherency of the generated output. In contrast, the utilization of local padding in the generator effectively mitigates these issues, resulting in a visually consistent and coherent image as shown in Figure 6.

We also studied the effect of having a fully convolutional generator instead of a traditional generator that uses a fully connected input layer followed by convolutional layers similar to [18]. The results in Figure 12 show that the fully convolutional generator is able to generate diverse and visually appealing textures, while the generator with a fully connected layer suffers from spatial mode collapse, producing less varied textures.

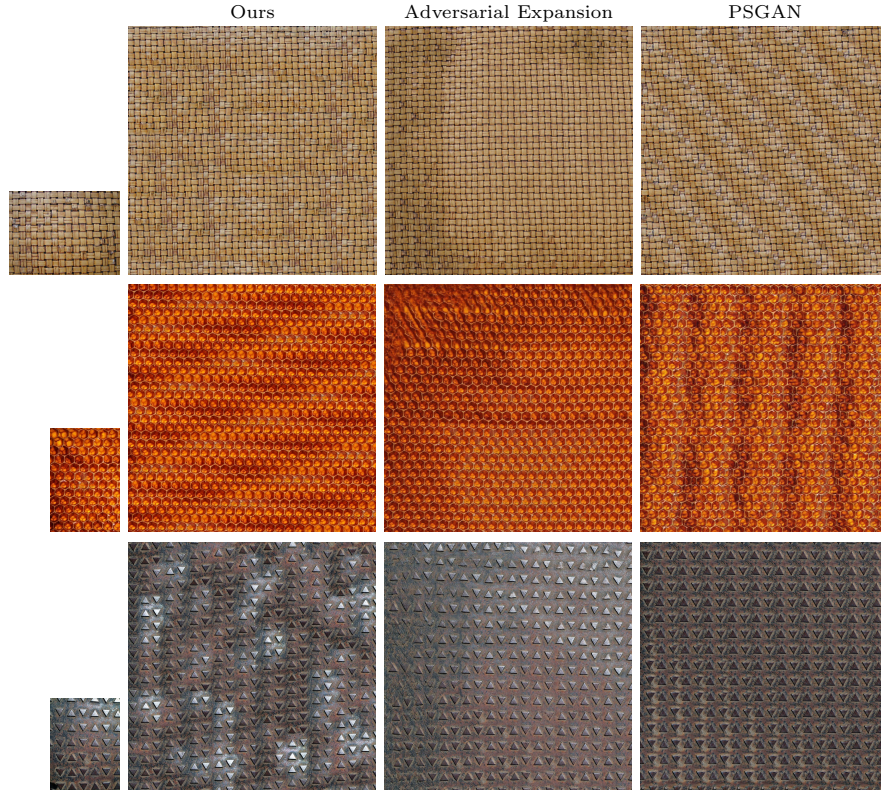


Figure 9: Regular textures generated by the proposed method with periodic inputs, adversarial expansion and PSGAN. While the stochastic variations of Adversarial Expansion and PSGAN are low across the spatial domain, our models were able to generate images that maintained the regular patterns in the original examples while also being diverse.

**Method limitations.** The proposed method for generating texture images of arbitrary size represents a promising scalable solution in the field of texture synthesis. However, there are several limitations to be considered. One limitation of the method is its inability to effectively generate non-stationary textures since the patch-based generation does not take into account the non-stationary variations in the spatial domain as shown in Figure 13. Moreover, because of the autoregressive nature of the model, redundant computations are performed as patches are regenerated with the correct padding. Furthermore, the method requires storing a fraction of the activations to be used for local padding in the regenerated patches.

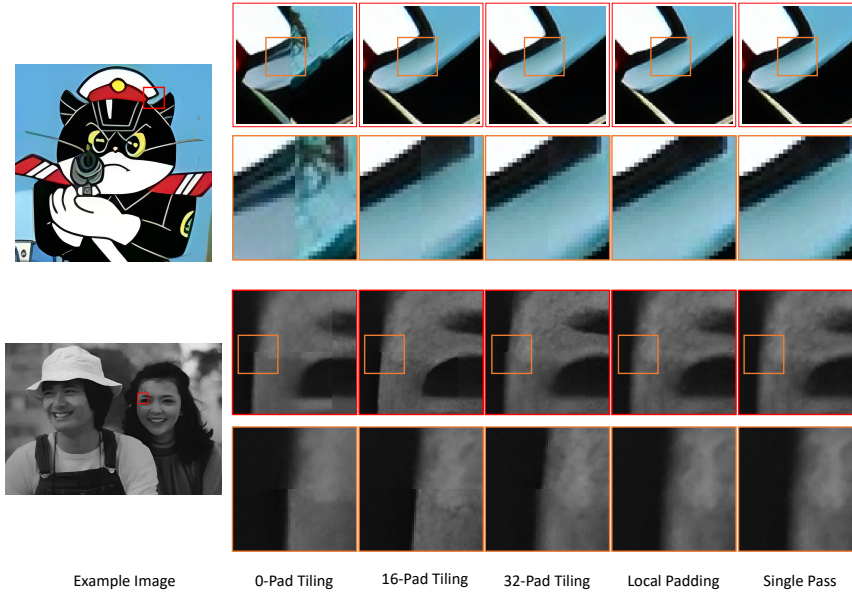


Figure 10: Applications of local padding in super-resolution. Two examples of super-resolved images using Real-ESRGAN model. The input images are processed using tiling with different overlapping sizes and local padding. The results are compared to passing the inputs to the model in a single shot.



Figure 11: Two examples of texture images generated using zero-padding instead of local padding. The images illustrate how zero-padding leads to visible seaming artifacts between the patches.

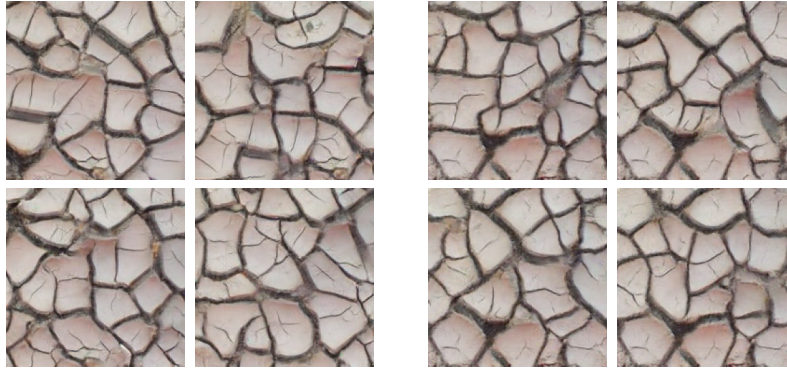


Figure 12: Comparison of texture generated using a fully convolutional generator (left) versus a generator with a fully connected layer (right). The fully convolutional generator demonstrates diverse texture samples, whereas the generator with a fully connected layer suffers from spatial mode collapse, producing less varied textures, as evidenced in areas such as the bottom left corners.

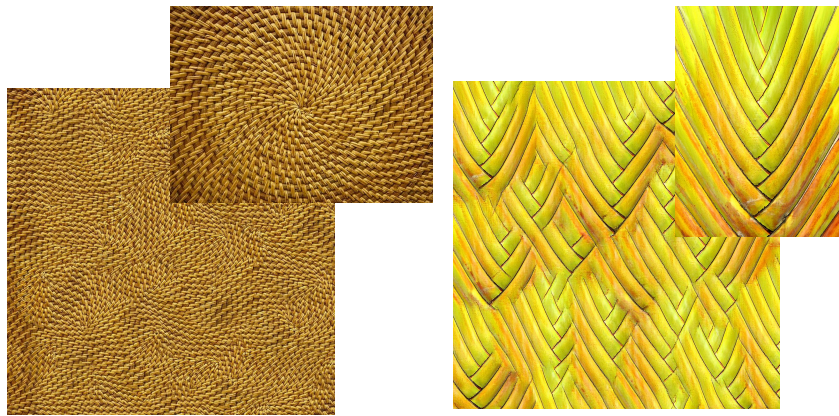


Figure 13: The method failure to maintain the non-stationarity in the original textures (top right). As the model only uses the information at the border of the image to assemble the patches, it fails to capture the non-stationary patterns.

## 5 Conclusion

We have presented a novel approach for synthesizing textures of infinite sizes trained on a single texture image. The proposed patch-based generation with local padding addresses the limitation of memory scalability and the generation



of high-quality and diverse large size textures, that have challenged previous methods. The trained models successfully generate visually appealing texture images with intricate details and seamless transitions between patches. Infinite-size textures can also be synthesized by incremental generation in a scalable way without a proportional growth in GPU memory. Nevertheless, this approach has its limitations, including the requirements to cache a fraction of the feature maps in the scaling steps and the inability to handle non-stationary textures.

## 6 Acknowledgment

The first author thanks TotalEnergies for the financial support. The authors acknowledge TotalEnergies for authorizing the publication of this paper.

## References

- [1] I. Goodfellow, J. Pouget-Abadie, M. Mirza, B. Xu, D. Warde-Farley, S. Ozair, A. Courville, and Y. Bengio, “Generative adversarial nets,” in *Advances in neural information processing systems*, pp. 2672–2680, 2014.
- [2] N. Jetchev, U. Bergmann, and R. Vollgraf, “Texture synthesis with spatial generative adversarial networks,” *arXiv preprint arXiv:1611.08207*, 2016.
- [3] U. Bergmann, N. Jetchev, and R. Vollgraf, “Learning texture manifolds with the periodic spatial gan,” *arXiv preprint arXiv:1705.06566*, 2017.
- [4] Y. Zhou, Z. Zhu, X. Bai, D. Lischinski, D. Cohen-Or, and H. Huang, “Non-stationary texture synthesis by adversarial expansion,” *arXiv preprint arXiv:1805.04487*, 2018.
- [5] T. R. Shaham, T. Dekel, and T. Michaeli, “Singan: Learning a generative model from a single natural image,” in *Proceedings of the IEEE/CVF International Conference on Computer Vision*, pp. 4570–4580, 2019.
- [6] T. de Bel, M. Hermsen, J. Kers, J. van der Laak, and G. Litjens, “Stain-transforming cycle-consistent generative adversarial networks for improved segmentation of renal histopathology,” 2018.
- [7] M. Böhlend, R. Bruch, S. Bäuerle, L. Rettenberger, and M. Reischl, “Improving generative adversarial networks for patch-based unpaired image-to-image translation,” *IEEE Access*, vol. 11, pp. 127895–127906, 2023.
- [8] X. Wang, L. Xie, C. Dong, and Y. Shan, “Real-esrgan: Training real-world blind super-resolution with pure synthetic data,” in *Proceedings of the IEEE/CVF international conference on computer vision*, pp. 1905–1914, 2021.

- [9] J.-Y. Zhu, T. Park, P. Isola, and A. A. Efros, “Unpaired image-to-image translation using cycle-consistent adversarial networks,” in *Proceedings of the IEEE international conference on computer vision*, pp. 2223–2232, 2017.
- [10] Y. Tian, X. Peng, L. Zhao, S. Zhang, and D. N. Metaxas, “Cr-gan: learning complete representations for multi-view generation,” *arXiv preprint arXiv:1806.11191*, 2018.
- [11] L. Zhao, X. Peng, Y. Tian, M. Kapadia, and D. N. Metaxas, “Towards image-to-video translation: A structure-aware approach via multi-stage generative adversarial networks,” *International Journal of Computer Vision*, vol. 128, pp. 2514–2533, 2020.
- [12] C. Ledig, L. Theis, F. Huszár, J. Caballero, A. Cunningham, A. Acosta, A. Aitken, A. Tejani, J. Totz, Z. Wang, *et al.*, “Photo-realistic single image super-resolution using a generative adversarial network,” in *Proceedings of the IEEE conference on computer vision and pattern recognition*, pp. 4681–4690, 2017.
- [13] K. Zhang, J. Liang, L. Van Gool, and R. Timofte, “Designing a practical degradation model for deep blind image super-resolution,” in *Proceedings of the IEEE/CVF International Conference on Computer Vision*, pp. 4791–4800, 2021.
- [14] D. Pathak, P. Krahenbuhl, J. Donahue, T. Darrell, and A. A. Efros, “Context encoders: Feature learning by inpainting,” in *Proceedings of the IEEE conference on computer vision and pattern recognition*, pp. 2536–2544, 2016.
- [15] J. Yu, Z. Lin, J. Yang, X. Shen, X. Lu, and T. S. Huang, “Generative image inpainting with contextual attention,” in *Proceedings of the IEEE conference on computer vision and pattern recognition*, pp. 5505–5514, 2018.
- [16] A. Radford, L. Metz, and S. Chintala, “Unsupervised representation learning with deep convolutional generative adversarial networks,” *arXiv preprint arXiv:1511.06434*, 2015.
- [17] A. Frühstück, I. Alhashim, and P. Wonka, “Tilegan: synthesis of large-scale non-homogeneous textures,” *ACM Transactions on Graphics (ToG)*, vol. 38, no. 4, pp. 1–11, 2019.
- [18] A. Brock, J. Donahue, and K. Simonyan, “Large scale GAN training for high fidelity natural image synthesis,” *arXiv preprint arXiv:1809.11096*, 2018.
- [19] T. Karras, S. Laine, and T. Aila, “A style-based generator architecture for generative adversarial networks,” in *Proceedings of the IEEE/CVF conference on computer vision and pattern recognition*, pp. 4401–4410, 2019.

- [20] T. Karras, S. Laine, M. Aittala, J. Hellsten, J. Lehtinen, and T. Aila, “Analyzing and improving the image quality of stylegan,” in *Proceedings of the IEEE/CVF conference on computer vision and pattern recognition*, pp. 8110–8119, 2020.
- [21] T. Karras, M. Aittala, S. Laine, E. Härkönen, J. Hellsten, J. Lehtinen, and T. Aila, “Alias-free generative adversarial networks,” *Advances in Neural Information Processing Systems*, vol. 34, 2021.
- [22] L. Zhao, Z. Zhang, T. Chen, D. Metaxas, and H. Zhang, “Improved transformer for high-resolution gans,” *Advances in Neural Information Processing Systems*, vol. 34, pp. 18367–18380, 2021.
- [23] H. Pinckaers, B. Van Ginneken, and G. Litjens, “Streaming convolutional neural networks for end-to-end learning with multi-megapixel images,” *IEEE transactions on pattern analysis and machine intelligence*, vol. 44, no. 3, pp. 1581–1590, 2020.
- [24] C. H. Lin, C.-C. Chang, Y.-S. Chen, D.-C. Juan, W. Wei, and H.-T. Chen, “COCO-GAN: Generation by parts via conditional coordinating,” in *Proceedings of the IEEE/CVF international conference on computer vision*, pp. 4512–4521, 2019.
- [25] C. H. Lin, H.-Y. Lee, Y.-C. Cheng, S. Tulyakov, and M.-H. Yang, “Infinitygan: Towards infinite-pixel image synthesis,” *arXiv preprint arXiv:2104.03963*, 2021.
- [26] R. Liu, J. Lehman, P. Molino, F. Petroski Such, E. Frank, A. Sergeev, and J. Yosinski, “An intriguing failing of convolutional neural networks and the coordconv solution,” *Advances in neural information processing systems*, vol. 31, 2018.
- [27] Ł. Struski, S. Knop, P. Spurek, W. Daniec, and J. Tabor, “Locogan—locally convolutional gan,” *Computer Vision and Image Understanding*, vol. 221, p. 103462, 2022.
- [28] I. Skorokhodov, G. Sotnikov, and M. Elhoseiny, “Aligning latent and image spaces to connect the unconnectable,” in *Proceedings of the IEEE/CVF International Conference on Computer Vision*, pp. 14144–14153, 2021.
- [29] X. Huang and S. Belongie, “Arbitrary style transfer in real-time with adaptive instance normalization,” in *Proceedings of the IEEE international conference on computer vision*, pp. 1501–1510, 2017.
- [30] K. He, X. Zhang, S. Ren, and J. Sun, “Deep residual learning for image recognition,” in *Proceedings of the IEEE conference on computer vision and pattern recognition*, pp. 770–778, 2016.

- [31] P. Isola, J.-Y. Zhu, T. Zhou, and A. A. Efros, “Image-to-image translation with conditional adversarial networks,” in *Proceedings of the IEEE conference on computer vision and pattern recognition*, pp. 1125–1134, 2017.
- [32] T. Park, M.-Y. Liu, T.-C. Wang, and J.-Y. Zhu, “Semantic image synthesis with spatially-adaptive normalization,” in *Proceedings of the IEEE Conference on Computer Vision and Pattern Recognition*, pp. 2337–2346, 2019.
- [33] T. Miyato, T. Kataoka, M. Koyama, and Y. Yoshida, “Spectral normalization for generative adversarial networks,” *arXiv preprint arXiv:1802.05957*, 2018.
- [34] D. P. Kingma and J. Ba, “Adam: A method for stochastic optimization,” *arXiv preprint arXiv:1412.6980*, 2014.